

A Study of the Chemical Structure of Laminar Premixed HC(O)OH/O₂/Ar Flames at 1 atm

K.N. Osipova^{1,2}, S. Mani Sarathy³, O.P. Korobeinichev¹ and A.G. Shmakov^{1,2 a)}

¹*Voevodsky Institute of Chemical Kinetics and Combustion SB RAS, Novosibirsk 630090, Russia*

²*Novosibirsk State University, Novosibirsk 630090, Russia*

³*King Abdullah University of Science and Technology, Clean Combustion Research Center, Physical Sciences and Engineering Division, Thuwal, Kingdom of Saudi Arabia*

^{a)}shmakov@kinetics.nsc.ru

Abstract. Flame structure of laminar premixed HC(O)OH/O₂/Ar was studied both experimentally and numerically. Three available chemical kinetic models were tested. In general, all models agree with experimental results for H₂O, CO, O₂, CO₂, HC(O)OH within the experimental error. For most of the intermediates all the models well capture the peak position and concentration profiles shape.

INTRODUCTION

Nowadays energy supply systems are primarily based on fossil fuels. However, the combustion of such fuels produces high levels of CO₂ emissions, so the search of alternative fuels is a very important challenge [1]. Hydrogen is the most attractive candidate because hydrogen molecule contains no carbon atoms, thus CO and CO₂ are not produced. Hydrogen can be applied in power systems, for example, internal combustion engines and gas turbines.

Nevertheless, the direct use of hydrogen in engines has several technical difficulties associated with hydrogen storage, transportation and handling. For example, for engines operation, we need liquid or compressed hydrogen. To achieve this purpose high pressure (100-700 bar) and very low temperature (-235 °C) are needed [2]. It means that until these problems are solved hydrogen can not be considered as a potential fuel for transportation systems. Methods based on hydrogen adsorption have limitations in temperature and pressure range, thus, they are not perspective.

Another solution is to use so-called hydrogen carriers. Hydrogen carriers are chemical species with sufficiently high amount of hydrogen in molecules. Formic acid is among these species [1]. In contrast to hydrogen, formic acid has well-established transportation and storage systems. It is worthy to note that despite the fact that formic acid molecule contains carbon atom, the temperature of formic acid decomposition with hydrogen formation is lower compared to other small organic molecules. This results into lower CO emissions [3]. Moreover, systems developed for gasoline use can be adjusted for formic acid [1].

However, there are a few papers focused on formic acid combustion and oxidation chemistry study. The authors of paper [4] studied oxidation of formic acid, methane, methyl alcohol and formaldehyde in static thermal reactor. Formic acid oxidation was followed by slower pressure rise compared to other chemicals. Thus, this was the first experimental observation of slow reactivity of formic acid. Among gaseous products of formic acid oxidation carbon oxides, water vapor and free hydrogen were present. The next work [5] was focused on low- pressure oxidation of formic acid. The use of optical spectroscopy enabled to register spectrum of CO and bands corresponding to OH. No bands indicating presence of C₂, CH and HCO were observed. Laminar flame speed of formic acid/oxygen/nitrogen blends was measured in the work [6]. The range of equivalence ratio was from 0.6 to 1.2, temperature of unburned mixture was 433K. The values of flame speed were obtained using total area method.

Since formic acid has narrow flammability limits, flame propagation is possible only for blends with low amount of diluent.

The reactions of formic acid monomolecular decomposition were studied experimentally under low temperature in works [7, 8] and under high temperatures in works [9-12]. According to the obtained results formic acid mostly decomposes via reaction $\text{HC(O)OH}=\text{CO}+\text{H}_2\text{O}$ whereas the reaction $\text{HC(O)OH}=\text{CO}_2+\text{H}_2$ has lower contribution. The work [13] showed that the role of reactions $\text{HC(O)OH}=\text{H}+\text{C(O)OH}$, $\text{HC(O)OH}=\text{CO}_2+2\text{H}$, $\text{HC(O)OH}=\text{HC(O)}+\text{OH}$ and $\text{HC(O)OH}=\text{H}+\text{HC(O)O}$ is negligible.

Formic acid is an intermediate species of oxidation of heavier molecules, thus the sub-mechanism of formic acid oxidation is present in mechanisms developed for such fuels as ethanol [14], dimethyl ether [15], propane [16], acetic acid [17], butanoic and pentanoic acids [18].

There is only one theoretical work [19] focused on development of formic acid oxidation mechanism. Using quantum chemistry ab initio approach rate constants of reactions of formic acid with H, O and HO_2 radicals were calculated. Rate constants for other reactions were adopted from published papers. Modeling results were compared with experimental ones obtained in the work [6]. The best agreement was achieved for lean blends whereas for rich blends model overpredicted the values of laminar flame speed.

One of the most recent work on formic acid oxidation [20] presents flame speed measurements for formic acid/air blends at temperature of 373K and 423K as well as for formic acid/hydrogen/air and formic acid/hydrogen/carbon dioxide/air blends at 373K and 358K respectively. In this work the mechanism of formic acid oxidation was proposed. Reactions for $\text{C}_0\text{-C}_3$ hydrocarbons were adopted for Aramco2.0 mechanism [21] since this mechanism was widely tested. Reactions for formic acid were taken from the work [19]. Results showed that for formic acid/air blends at 373K the proposed mechanism has the same trend as described in the work [19]. However, for 423K the model underpredicts the values of burning velocity for lean and rich blends. For formic acid/hydrogen/air flames the best agreement was achieved for lean and rich systems. The paper has experimental data only for lean formic acid/hydrogen/carbon dioxide/air mixtures (equivalence ratio from 0.6 to 0.9). The closer are conditions to stoichiometric the better agreement provides the model.

Laminar burning velocities of formic acid/air blends were measured in another recent work [22] at temperatures 423 K and 453K. The authors tested mechanism developed by Glarborg et.al [19] and Aramco 3.0 mechanism [23]. It was revealed that Glarborg et al model provides good agreement for lean and rich blends while Aramco 3.0 overestimates the values of burning velocities. The trend of Glarborg et al model is different from that which was observed in works [19, 20].

Thus, there is a lack of experimental data on formic acid oxidation. In particular, there are no works on structure of formic acid flames. Since the development of reliable model strongly needs these experiments, the aim of the present work was to obtain new experimental data on formic acid/oxygen/argon flame structure at atmospheric pressure as well as the validation of published models.

EXPERIMENT

In this work we measured experimentally flame structure of stoichiometric formic acid/oxygen/argon blend (0.30/0.15/0.55) at atmospheric pressure. The flame was stabilized on Botha-Spalding flat burner with diameter 16 mm [24]. The volumetric flow rate was 40 cm^3/s (298K, 1 atm). In the experiment the temperature of the burner was 95°C. The premixed blend of formic acid, oxygen and argon came to the burner through evaporator. Liquid formic acid was supplied to evaporator with a syringe and a stepper motor. An evaporator is a pyrex vessel filled with metal beads. The temperature of evaporator in the experiment was kept at 80°C. The detailed description of burner, evaporator and fuel supply system is given in [25].

For gas sampling quartz conic probe with internal opening angle of 40° and orifice diameter of 0.08 was used. The wall thickness near the probe tip was also 0.08mm.

Chemical structure of formic acid/oxygen/argon flame was measured with molecular-beam mass-spectrometric setup with soft electron-impact ionization. The detailed description of experimental setup is provided in work [26]. In the current work the energy of ionizing electrons was 11.5-16.65eV.

In the most cases, soft ionization enables to avoid or at least minimize contribution of fragment ions of heavier compounds (usually of the fuel) to mass-spectrum of smaller species. Otherwise, the calibration procedure is applied. The calibration process includes measurement of peak intensities of the fuel under different values of ionizing electrons energy.

To recalculate peak intensities to mole fractions the next formula was used: $I=S*X$, where I is intensity, X -mole fraction and S -calibration coefficient. To obtain the value of S three methods were applied: 1) direct calibration; 2) mass-balance calibration; 3) method of relative ionization cross-sections [27]. The values of cross-sections were taken from the database [28]. If the value for particular species is not present in database, it was estimated with methods, proposed in [29, 30].

To consider gas-dynamic perturbations appearing because of probe presence experimental concentration profiles was shifted by the distance, estimated according to work [31]. In this work the shift value was 0.4 mm.

For temperature measurement we used thin S-type thermocouples (Pt-Pt10%Rh). Thermocouples were made from a wire with diameter of 0.03 mm and coated with SiO_2 . In temperature measurements the thermocouple was placed at 0.2 mm from the probe's tip.

MODELING

For numerical simulation the code PREMIX from CHEMKIN PRO package was applied. Experimentally measured temperature profile was used as an input data. We tested three available chemical kinetic mechanisms of formic acid oxidation: Glarborg et al., Konnov et al. and updated Aramco2.0. Table 1. summarizes the information about mechanisms applied. GRAD and CURV parameters were set as 0.1 and 0.2 respectively.

TABLE 1. Chemical kinetic mechanisms of formic acid oxidation

Mechanism	Species Number	Reactions Number	Reference	Model №
Glarborg et al	27	75	[19]	Model 1
Konnov et al	100	1140	[17]	Model 2
Updated Aramco2.0	305	1761	[20]	Model 3

RESULTS AND DISCUSSION

Figure 1. shows mole fraction profiles of reactants (HC(O)OH and O_2), main combustion products (H_2O , CO , CO_2), temperature profile as well as modelling results. In general, all models applied showed good predictive capability. According to Model 1 and Model 2 formic acid starts to oxidize a little bit earlier than it is observed in the experiment, but this difference is within the experimental uncertainty. Model 3 gave the closest result to the experiment. Mole fraction profiles of H_2O , CO and O_2 are well captured by all models. Model 2 better describes CO_2 than two other models.

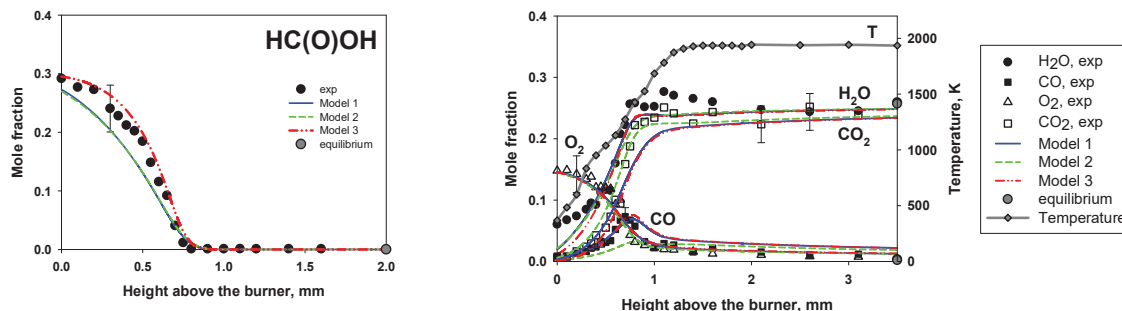


FIGURE 1. Reactants, main combustion product concentration profiles and temperature profile in $\text{HC(O)OH/O}_2/\text{Ar}$ flame

Figure 2. presents mole fraction profiles of intermediate species registered in $\text{HC(O)OH/O}_2/\text{Ar}$ flame. All models overestimate peak concentration of H . Peak position and profile's shape is predicted correctly.

Mole fraction profile of H_2 is better described by Model 2, whereas according to Model 1 and Model 3 the profile has two peaks. The reason is that for $\text{O}+\text{H}_2=\text{OH}+\text{H}$ reaction rate profile has two peaks according to Model 1 and Model 3. In Model 2 it has only one peak. In the experiment the second peak was not observed.

For O radical all models predict higher peak concentration than experimental one, Model 2 gives the closest value. In the case of OH concentration profile all models give almost the same results and overestimate the peak concentration.

Model 1 predicts the peak concentration of CH₂O to be $\sim 10^{-9}$ when the experimental value is $\sim 2.5 \cdot 10^{-4}$. For this reason modeling results with Model 1 are not given on the Fig.2. Model 2 predicts peak concentration to be around $2.5 \cdot 10^{-5}$ and according to Model 3 the value is $\sim 10^{-4}$. The reason of this difference is that in Model 2 and Model 3 there are reactions of CH₂O formation from formic acid. In particular, in Model 2 it is $\text{HC(O)OH} + \text{H} = \text{CH}_2\text{O} + \text{OH}$ and in Model 3 there are two reactions: $\text{HC(O)OH} + \text{H} = \text{HOCH}_2\text{O}$ and $\text{HOCH}_2\text{O} = \text{CH}_2\text{O} + \text{OH}$. Model 1 has no reactions of direct CH₂O formation from formic acid molecule.

All the models applied correctly predict the shape and peak position of HO₂ but overestimate peak value by around 3 times. For H₂O₂ peak value is strongly overestimated by all models. The difference is around 7 times. This indicates that the mechanism part of hydrogen peroxide oxidation needs to be refined.

C(O)OH and HC(O)O radicals were not registered experimentally, therefore only modeling results are presented. All the mechanisms give almost the same results.

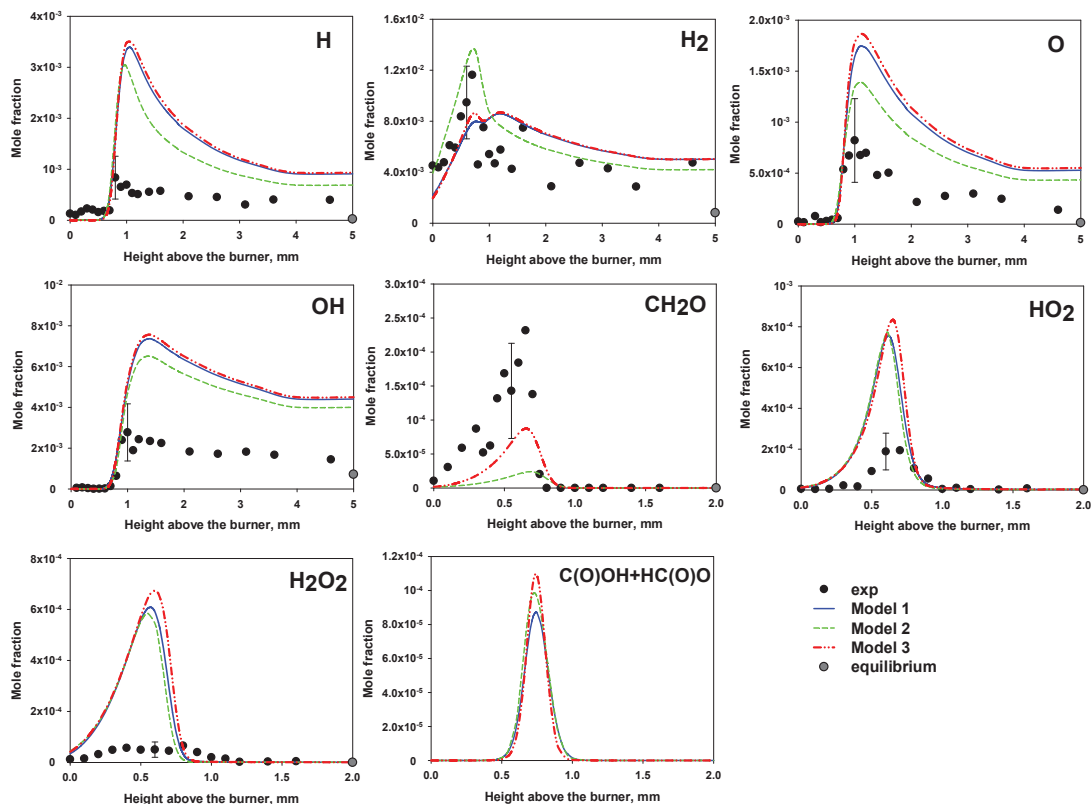


FIGURE 2. Intermediates concentration profiles in HC(O)OH/O₂/Ar flame

CONCLUSIONS

Three published chemical kinetic mechanisms of formic acid oxidation were tested against new experimental data on flame structure of HC(O)OH/O₂/Ar blend. In general, all the models applied demonstrated good predictive capability since they are able to reproduce mole fraction profiles of reactants and major combustion products within the experimental uncertainty and predict peak concentration and profiles shape for the most intermediates quite well.

All the models tend to overestimate peak concentration of H, O, OH, HO₂ and H₂O₂, for H₂O₂ this effect is more significant. Model 1 and Model 3 predict H₂ profile to have two peaks whereas according to the Model 2 it has only one peak which better agrees with experimental results. For CH₂O Model 1 gives the value of peak concentration around 4-5 orders lower than the experimental one. Model 3 provides the closest agreement.

ACKNOWLEDGMENTS

The research at King Abdullah University of Science and Technology (KAUST) was supported by Saudi Aramco

REFERENCES

1. J. Eppinger and K.-W. Huang, *ACS Energy Lett.* **2**(1), 188–195 (2017).
2. K. Sordakis, C. Tang, L. K. Vogt, H. Junge, P. J. Dyson, M. Beller and G. Laurency, *Chem. Rev.* **118**, 372–433 (2018).
3. X. Wang, Q. Meng, L. Gao, Z. Jin, J. Ge, C. Liu and W. Xing, *Int. J. Hydrog. Energy* **43**(14), 7055–7071 (2018).
4. W.A. Bone and J.B. Gardner, *Proc. Roy. Soc. Lond. A* **154**, 297–328 (1936).
5. A.G. Gaydon and H.G. Wolfhard, *Symp. Combust. Flame Explos. Phenom.* **3**(1), 504–518 (1949).
6. E. de Wilde and A. van Tiggelen, *Bull. Soc. Chim. Belges* **77**, 67–76 (1968).
7. P.G. Blake and C. Hinshelwood, *Proc. Roy. Soc. Lond.* **255**, 444–455 (1960).
8. P.G. Blake, H.H. Davies and G.E. Jackson, *J. Chem. Soc. B* **10**, 1923–1925 (1971).
9. D.S.Y. Hsu, W.M. Shaub, M. Blackburn and M.C. Lin, *Proc. Combust. Inst.* **19**, 89–96 (1982).
10. K. Saito, T. Kakumoto, H. Kuroda, S. Torii and A. Imamura, *J. Chem. Phys.* **80**, 4989–4996 (1984).
11. K. Saito, T. Shiose, O. Takahashi, Y. Hidaka, F. Aiba and K. Tabayashi, *J. Phys. Chem. A* **109**, 5352–5357 (2005).
12. A. Elwardany, E.F. Nasir, Et. Es-sebbar and A. Farooq, *Proc. Combust. Inst.* **35**, 429–436 (2015).
13. M. Klatt, M. Rohrig and H.G. Wagner, *Z. Naturforsch* **47**, 1138–1140 (1992).
14. N.M. Marinov, *Int. J. Chem. Kin.* **31**, 183–220 (1999).
15. S.L. Fischer, F.L. Dryer and H.J. Curran, *Int. J. Chem. Kin.* **32**, 713–740 (2000).
16. F. Battin-Leclerc, A.A. Konnov, J.L. Jaffrezo and M. Legrand, *Combust. Sci. Technol.* **180**, 343–370 (2007).
17. M. Christensen and A. A. Konnov, *Combust. Flame* **170**, 12–29 (2016).
18. S. Namysl, M. Pelucchi, O. Herbinet, A. Frassoldati, T. Faravelli and F. Battin-Leclerc, *Chem. Eng. J.* **373**, 973–984 (2019).
19. P. Marshall and P. Glarborg, *Proc. Combust. Inst.* **35**, 153–160 (2015).
20. S. M. Sarathy, P. Brequigny, A. Katoch, A.M. Elbaz, W. L. Roberts, R. W. Dibble and F. Foucher, *Energ. Fuel.* **34**(6), 7564–7572 (2020).
21. Saudi Aramco mechanism release v. 2.0, Combustion Chemistry Centre, National University of Ireland, Galway, (2016).
22. G. Yin, Q. Gao, E. Hu, J. Xu, M. Zhou and Z. Huang, *Combust. Flame* **220**, 73–81 (2020).
23. Saudi Aramco mechanism release v. 3.0, Combustion Chemistry Centre, National University of Ireland, Galway, (2018).
24. J. P. Botha and D. B. Spalding, *Proc. Roy. Soc. Lond.* **255**, 71–96 (1954).
25. K. N. Osipova, T. A. Bolshova, O. P. Korobeinichev, L. V. Kuibida and A. G. Shmakov, *Energ. Fuel.* **33**, 4585–4597 (2019).
26. A. M. Dmitriev, K. N. Osipova, D. A. Knyazkov, I. E. Gerasimov, A. G. Shmakov and O. P. Korobeinichev, *Combust. Explos. Shock Waves* **54**, 125–135 (2018).
27. T.A. Cool, K. Nakajima, K.A. Taatjes, A. McIlroy, P.R. Westmoreland, M.E. Law and A. Morel, *Proc. Combust. Inst.* **30**, 1681–1688 (2005).
28. <https://physics.nist.gov/PhysRefData/Ionization/molTable.html>
29. A. Lamprecht, B. Atakan and K. Kohse-Hoeinghaus, *Combust. Flame* **122**, 483–491 (2000).
30. W. L. Fitch and A. D. Sauter, *Anal. Chem.* **55**, 832–835, (1983).
31. I. E. Gerasimov, D. A. Knyazkov, S. A. Yakimov, T. A. Bolshova, A. G. Shmakov and O. P. Korobeinichev, *Combust. Flame* **159**, 1840–1850 (2012).